Ion-Permselective pH-Switchable Mesoporous Silica Thin Layers

Dina Fattakhova-Rohlfing,[†,*] Michael Wark,[‡] and Jiří Rathouský[§]

Department of Physical Chemistry and Biochemistry, Ludwig-Maximilians-Universität Munich, Butenandtstrasse 5-13 (E), 81377 Munich, Germany, Institute of Physical Chemistry and Electrochemistry, Gottfried Wilhelm Leibniz Universität Hannover, Callinstrasse 3-3a, 30167 Hannover, Germany, and J. Heyrovský Institute of Physical Chemistry, Academy of Sciences of the Czech Republic, Dolejškova 3, 18223 Prague 8, Czech Republic

Received October 6, 2006. Revised Manuscript Received December 21, 2006

Organized mesoporous layers of SiO_2 with narrow pore size distribution centered at ca. 7 nm, which were uniformly functionalized with readily protonated amino groups, exhibit excellent permselective membrane properties. Their selectivity and permeability can be reversibly controlled by changing pH. The flux of hexacyanoferrate $Fe(CN)_6^{3-}$ anions, hexaamino-ruthenium $Ru(NH_3)_6^{3+}$ cations, and neutral ferrocene methanol molecules through the amino functionalized silica layers was monitored by cyclic voltammetry at different solution pH values. Depending on their charges, the flux of ions can be completely blocked or enhanced, while the permeation of uncharged species is affected adversely only in a limited extent by the change in pH. The high membrane porosity ensures fast penetration rates of the analytes and much faster response to the changes in pH compared to those of typical compact organic polymer layers. As the amino functionalized mesoporous silica layers enable the efficient separation of differently charged species from complex mixtures, they are attractive for applications in biology and medicine, where such mixtures are often encountered, e.g., for the separation of blood, urine, or sera components.

1. Introduction

Smart membranes, whose permeability and selectivity can be easily controlled by changing some simple process parameter, e.g., illumination, temperature, or concentration, are of major importance in a number of advanced technologies, such as switchable devices for selective separation, analysis, and sensorics.[1−8] Most frequently, the performance of the layers is controlled by pH.[6,9−17] The control mechanism is based on the excess positive or negative charge generated on anchored functional groups due to the change in solution pH, which makes the layers selective to negatively or positively charged species, respectively. Most frequently, a polymer matrix is used as the support for pH-sensitive functional groups. A number of pH-responsive membranes have been developed based on, e.g., organic polymer layers obtained by the layer-by-layer deposition[16,18] or the polymer casting on a support[19,20] and the sol−gel films prepared from organosilanes.[21−23] Polymer-based membranes, exhibiting very high selectivity, can be prepared in mild conditions on any kind of substrate. On the other hand, they suffer from a number of drawbacks, especially generally low and poorly defined porosity, which drastically slows down the rate of penetration. Further they exhibit low stability especially in organic solvents and swelling of organic polymers, which changes uncontrollably their permeation properties. Recently, silica-based opal layers were proposed as a robust inorganic matrix for the preparation of pH-responsive layers.[24] The opal-based membranes exhibit excellent porosity ensuring fast penetration rates of the analytes but, on the other hand, much lower selectivity due to the large pore size in macropore range. Also, their difficult scaling up and low mechanical stability, as they are composed of single spheres,

* To whom correspondence should be addressed. E-mail: Dina.Fattakhova@cup.uni-muenchen.de.
† Ludwig-Maximilians-Universität Munich.
‡ Gottfried Wilhelm Leibniz Universität Hannover.
§ J. Heyrovský Institute of Physical Chemistry.

(1) Nishizawa, M.; Menon, V. P.; Martin, C. R. *Science* **1995**, *268*, 700.
(2) Yu, S. F.; Lee, S. B.; Martin, C. R. *Anal. Chem.* **2003**, *75*, 1239.
(3) Steinle, E. D.; Mitchell, D. T.; Wirtz, M.; Lee, S. B.; Young, V. Y.; Martin, C. R. *Anal. Chem.* **2002**, *74*, 2416.
(4) Jirage, K. B.; Martin, C. R. *Trends Biotechnol.* **1999**, *17*, 197.
(5) Ito, T.; Hioki, T.; Yamaguchi, T.; Shinbo, T.; Nakao, S.; Kimura, S. *J. Am. Chem. Soc.* **2002**, *124*, 7840.
(6) Liu, Y. L.; Zhao, M. Q.; Bergbreiter, D. E.; Crooks, R. M. *J. Am. Chem. Soc.* **1997**, *119*, 8720.
(7) Rao, G. V. R.; Krug, M. E.; Balamurugan, S.; Xu, H. F.; Xu, Q.; Lopez, G. P. *Chem. Mater.* **2002**, *14*, 5075.
(8) Tokarev, I.; Orlov, M.; Minko, S. *Adv. Mater.* **2006**, *18*, 2458.
(9) Lee, S. B.; Martin, C. R. *Anal. Chem.* **2001**, *73*, 768.
(10) Minagawa, M.; Tanioka, A. *J. Colloid Interface Sci.* **1998**, *202*, 149.
(11) Minagawa, M.; Tanioka, A.; Ramirez, P.; Mafe, S. *J. Colloid Interface Sci.* **1997**, *188*, 176.
(12) Chun, K. Y.; Stroeve, P. *Langmuir* **2002**, *18*, 4653.
(13) Wan, K. W.; Malgesini, B.; Verpilio, L.; Ferruti, P.; Griffiths, P. C.; Paul, A.; Hann, A. C.; Duncan, R. *Biomacromolecules* **2004**, *5*, 1102.
(14) Julbe, A.; Farrusseng, D.; Guizard, C. *Sep. Purif. Technol.* **2001**, *25*, 11.
(15) Jimbo, T.; Ramirez, P.; Tanioka, A.; Mafe, S.; Minoura, N. *J. Colloid Interface Sci.* **2000**, *225*, 447.
(16) Miller, S. A.; Martin, C. R. *J. Am. Chem. Soc.* **2004**, *126*, 6226.
(17) Ramirez, P.; Mafe, S.; Alcaraz, A.; Cervera, J. *J. Phys. Chem.* B **2003**, *107*, 13178.
(18) Park, M. K.; Deng, S. X.; Advincula, R. C. *J. Am. Chem. Soc.* **2004**, *126*, 13723.
(19) Ying, L.; Yu, W. H.; Kang, E. T.; Neoh, K. G. *Langmuir* **2004**, *20*, 6032.
(20) Martin, C. R.; Rubinstein, I.; Bard, A. J. *J. Am. Chem. Soc.* **1982**, *104*, 4817.
(21) Wei, H. J.; Collinson, M. M. *Anal. Chim. Acta* **1999**, *397*, 113.
(22) Hsueh, C. C.; Collinson, M. M. *J. Electroanal. Chem.* **1997**, *420*, 243.
(23) Collinson, M. M. *Trac-Trends in Analytical Chemistry* **2002**, *21*, 30.
(24) Newton, M. R.; Bohaty, A. K.; White, H. S.; Zharov, I. *J. Am. Chem. Soc.* **2005**, *127*, 7268.

10.1021/cm062389g CCC: $37.00
Published on Web 03/13/2007

make the practical application of such membranes far from straightforward.

In order to overcome the mentioned drawbacks, we propose functional layers based on mesoporous inorganic SiO_2 films as the permselective pH-switchable membranes. Such films can be prepared by the template-assisted sol−gel technique, which enables one to obtain functional layers with high and defined porosity with the pore size variable from the micropore to macropore range of 1−2 nm to 30−50 nm, respectively, by the selection of a template.[25−27] Highly robust and optically transparent layers, whose thickness is easy to control, can be deposited on supports of any kind and size. By postsynthetic grafting, almost any functionality can be introduced without any substantial distortion of the layer porosity.[28,29] These exclusive features of mesoporous films render them very attractive for the application as membrane layers. The suitable pore size ensuring good selectivity without diffusion restrictions gives them important advantage.[30] Moreover, the open porosity could provide the selective control exclusively over charged species while remaining permeable for the uncharged ones.

In this article, mesoporous films of amorphous SiO_2 postsynthetically functionalized with readily protonated amino groups[31] were studied as the pH-controllable ion-selective membrane layers. For the monitoring of the layer permeability, redox active ions, namely anionic hexacyanoferrate $Fe(CN)_6^{3-}$, cationic hexaaminoruthenium $Ru(NH_3)_6^{3+}$, and neutral ferrocene methanol FcOH, were used as analyte species. As the mentioned species have comparable size of 5 ± 0.5 Å,[32] only the difference in their charge is expected to influence their permeation behavior, while consideration of the molecule size effect can be practically omitted. This makes them very convenient and frequently used probes for testing pH-responsive membrane layers. The flux of the ionic redox species through the mesoporous layer was directly measured as the height of their voltammetric signal on conductive FTO-coated glass as a support.

2. Experimental Details

The preparation of silica films was carried out according to a template-assisted procedure using the Pluronic F127 (BASF) block copolymer as a structure directing agent (SDA).[33] All the chemicals used were purchased from Aldrich. A total of 10 mmol of SDA dissolved in 25 mL of ethanol was added to a solution of prehydrolyzed tetraethylorthosilicate (TEOS) prepared by refluxing the mixture of 10.4 g of TEOS in 33.3 mL of ethanol, 2.2 mL of water, and 5 mL of 0.1 M HCl for 1 h. The combined mixture was stirred for another 2 h. The final molar ratio of the components was TEOS/SDA/water/HCl/ethanol = 1/0.01/8/0.01/20. The films were deposited by dip-coating on a conducting F-doped tin oxide-coated glass substrate (FTO, AI Glass Corp. Japan, 9−15 Ohm/square) at the withdrawal rate of 70 mm min^{-1} at relative humidity of 40%, dried for 30 min at room temperature at relative humidity of 40%, and calcined at 400 °C for 4 h (temperature ramp of 0.8 °C min^{-1}) in order to remove the SDA. The FTO/glass slides (26 mm × 76 mm) were cleaned prior to the deposition by the consecutive sonication in a 5% solution of detergent LR-F (Qualilab), ethanol, and acetone.

The calcined silica films were functionalized by silylation with aminopropyltriethoxysilane (APTES). The silica-coated glass slides dried at 100 °C were treated with a 20 mmol L^{-1} solution of APTES in dichloromethane for 4 h at room temperature in a Schlenk flask equipped with a Teflon holder with a magnetic stirrer. In a subsequent step, the samples were washed by repeated vigorous stirring in dichloromethane and ethanol and dried at 80 °C.

Scanning transmission electron microscopy (STEM) was performed at 200 kV on a field-emission instrument (Jeol JEM-2100F UHR) employing high-angle annular dark-field contrast. The film thickness was measured by profilometry (Dektak). Texture characteristics of the films were determined by the analysis of adsorption isotherms of Kr at the boiling point of liquid nitrogen (approximately 77 K) using an ASAP 2010 apparatus (Micromeritics). For materials with very low surface area in the range of tens of cm^2—as is the case with thin porous films—an adsorptive with lower saturation vapor pressure than the routinely used nitrogen should be used since it reduces the uncertainty associated with the equipment dead volume. With this end in view, krypton adsorption at the boiling point of liquid nitrogen is mostly used for the determination of the surface area. The isotherms were measured on the films using special adsorption cells. Prior to each adsorption measurement, samples were outgassed at 150 °C over night, this temperature being the upper limit of the stability of the organic compounds used. The surface area of the mesoporous electrodes was determined by the BET method, the molecular area for krypton being taken as 0.21 nm^2. To make the data comparable, the BET surface area was converted to the surface area in $m^2\ g^{-1}$ and the specific surface area in $cm^2\ cm^{-2}$, which is the ratio of the total surface areas of the film and the substrate. The mass of the films was determined by weighing the substrate before and after the film preparation. The Raman spectra were recorded with a LabRAM HR UV−vis (Horiba Jobin Yvon) Raman microscope (Olympus BX41) with Symphony CCD detection system using a 632.81 nm laser. The spectra were taken from the powder scratched from the substrate. X-ray diffraction analysis was carried out in reflection mode by a Scintag XDS 2000 (Scintag Inc.) with Ni-filtered Cu Kα-radiation.

Electrochemical measurements were carried out using Autolab 12 potentiostat/galvanostat (Eco Chemie) with the GPES software for the collection and analysis of the data. Silica films on FTO glass used as working electrodes were masked with adhesive tape with an exposed area of 0.5 cm^2. The measurements were performed on several films to ensure the reproducibility of the results. Pt wire and silver/silver chloride/sat. KCl were taken as the auxiliary and reference electrodes, respectively. The cyclic voltammograms were taken in the range of scan rates from 20 mV s^{-1} to 2000 mV s^{-1}. The cyclic voltammograms in the text of the manuscript correspond to 200 mV/s if not specially noted. Buffered 0.1 M solution of KCl was employed as an electrolyte using a KH_2PO_4/Na_2HPO_4 pH 7 buffer (VWR), the pH being adjusted by 1 M solution of KOH and HCl, respectively.

(25) Soler-Illia, G.; Innocenzi, P. *Chem.-Eur. J.* **2006**, *12*, 4478.
(26) Zhao, D. Y.; Huo, Q. S.; Feng, J. L.; Chmelka, B. F.; Stucky, G. D. *J. Am. Chem. Soc.* **1998**, *120*, 6024.
(27) Nicole, L.; Boissiere, C.; Grosso, D.; Quach, A.; Sanchez, C. *J. Mater. Chem.* **2005**, *15*, 3598.
(28) Angelome, P. C.; Soler-Illia, G. *Chem. Mater.* **2005**, *17*, 322.
(29) Yoshida, W.; Castro, R. P.; Jou, J. D.; Cohen, Y. *Langmuir* **2001**, *17*, 5882.
(30) Etienne, M.; Walcarius, A. *Electrochem. Commun.* **2005**, *7*, 1449.
(31) Rohlfing, D. F.; Rathousky, J.; Rohlfing, Y.; Bartels, O.; Wark, M. *Langmuir* **2005**, *21*, 11320.
(32) Zhang, J. L.; Williams, M. E.; Keefe, M. H.; Morris, G. A.; Nguyen, S. T.; Hupp, J. T. *Electrochem. Solid State Lett.* **2002**, *5*, E25.
(33) Zhao, D.; Yang, P.; Melosh, N.; Feng, J.; Chmelka, B. F.; Stucky, G. D. *Adv. Mater.* **1998**, *10*, 1380.

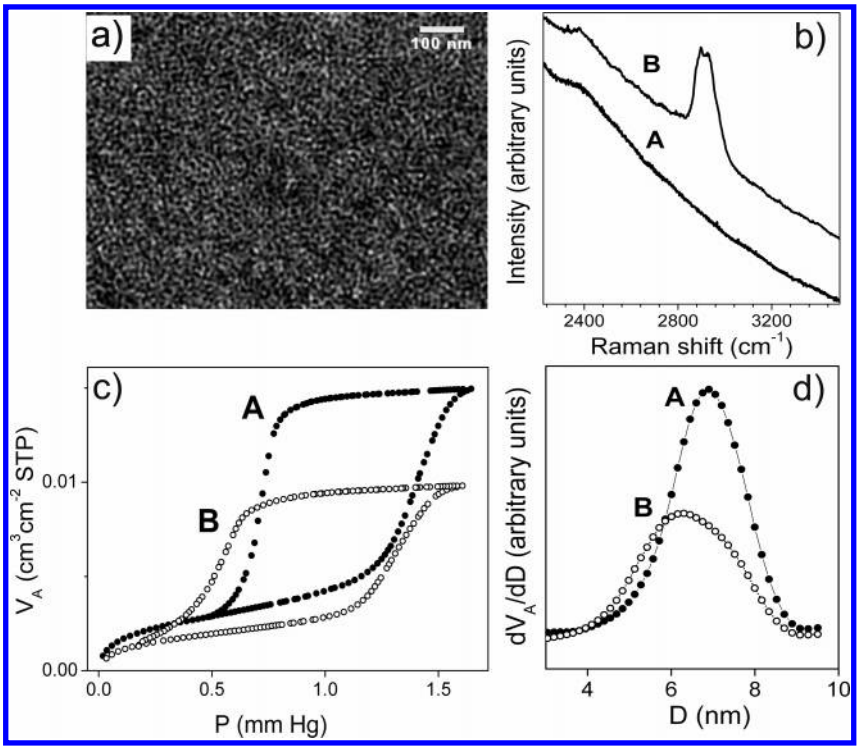

Figure 1. (a) Scanning transmission electron microscopy (STEM) image of the APTES-functionalized mesoporous SiO_2 film. (b) Raman spectra. (c) Adsorption isotherms of Kr at 77 K. (d) The pore size distribution for mesoporous SiO_2 films. In b−d, A and B are related to mesoporous films before and after the postsynthetic functionalization with APTES.

3. Results and Discussion

3.1. Preparation and Functionalization of Silica Films. The films of SiO_2 obtained after the template removal by calcination at 400 °C are highly transparent, homogeneous, and crack-free, as was confirmed by scanning electron microscopy (SEM) and optical microscopy. Transmission electron microscopy (TEM) (Figure 1a), SEM, Kr adsorption data (Figure 1c,d) and XRD patterns at small angles (Figure 1, Supporting Information) reveal the highly pronounced mesoporosity of the films. Generally, the pore size is reasonably uniform with narrow pore size distribution. However, the arrangement of the pore openings does not exhibit long-range ordering, with only some short-range order being discernible. The average pore diameter, porosity, specific surface area per cm^2 of the substrate, and BET surface area per 1 g of nonfunctionalized SiO_2 film determined from the adsorption data are 6.9 nm, 60%, 122 cm^2 cm^{-2}, and 435 m^2 g^{-1}, respectively, for a typical film 340 nm in thickness.

Silylation of mesoporous silica films with aminopropyltriethoxysilane (APTES) leads to the functionalization of silica surface with aminopropyl-moieties. This is clearly evidenced by the Raman spectra, which indicate the appearance of the $-CH_2-$ groups due to the presence of the aminopropyl chain after the silylation with APTES (Figure 1b). The quality of the postsynthetic chemical modification of the mesoporous silica films was tested by Kr adsorption measurements. As expected, the pore size and film porosity decrease after silylation with APTES, but at the same time the pore size distribution remains narrow (Figure 1c,d). This follows from the unchanged shape of the hysteresis loop for the silylated film in comparison with the pristine one. The desorption branch for the modified film is clearly shifted to the lower pressure range due to the decrease in the pore size. However, its steepness was only slightly affected, i.e., the narrowness of the pore size distribution was practically preserved. This indicates that the silylation agent is grafted homogeneously to the pore walls without blocking the pore volume and pore mouths and without any polymerization inside the pores. The average pore diameter, porosity, and specific surface area of the functionalized silica film are 6.3 nm, 39%, 82 cm^2 cm^{-2}, and 292 m^2 g^{-1}, respectively.

3.2. Permeation Properties of Mesoporous Silica Films. As can be seen from Figure 2, the 1 mmol L^{-1} solutions of $Fe(CN)_6^{3-}$, $Ru(NH_3)_6^{3+}$, and FcOH show similar voltammetric response on noncoated FTO electrode at pH 3, corresponding to a reversible one-electron-transfer reaction (Figure 2, A). The current response slightly decreases by ca. 20% at the electrodes coated with nonmodified mesoporous silica layers compared to the bare electrodes for all the redox probes (Figure 2, B), having practically no selectivity regarding the charge of the permeating ions.

The performance of the porous silica films drastically changes due to the functionalization of their surface with amino groups. At pH 3, the layer is highly permeable for the hexacyanoferrate anions, which is proved by the high detected current response (Figure 2, C). As no voltammetric signal of cations is observed, the silica film acts as a blocking layer for the flux of the hexaaminoruthenium cations at this pH. The flux of the neutral ferrocenemethanol molecules decreases compared to the nonfunctionalized silica film, but it remains significantly high at ca. 40%.

Monitoring of the voltammetric signal for all permeates in concentration of 1 mmol L^{-1} in the broad range of pH from 0.2 to 8.8 is presented in Figure 3 for all the three types of electrodes.

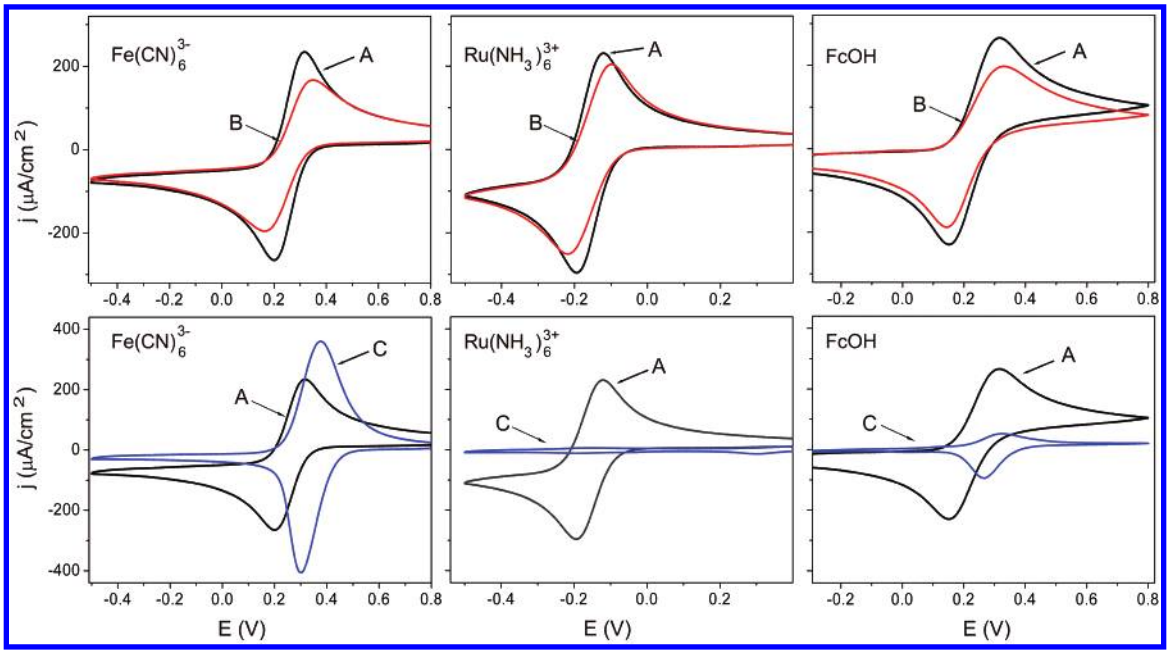

Figure 2. Voltammetric response of the FTO electrode: bare (A, black solid line) and coated with nonfunctionalized (B, red line) and APTES-functionalized (C, blue line) mesoporous SiO_2 films in 1 mmol L^{-1} solutions of potassium hexacyanoferrate (first column), hexaaminoruthenium chloride (second column), and ferrocenedimethanol (third column) at pH 3.

Hexacyanoferrate Anions. The voltammetric peak current of hexacyanoferrate anions on bare FTO electrode is not constant in this pH range due to its relatively slow pH-dependent electrode kinetics[34,35] and the negative charging of the surface of FTO electrode at high pH values creating an additional barrier to the electron-transfer reaction. The decrease in the current values with an increase in pH (Figure 3a, A) is accompanied by an increase in the potential difference between oxidation and reduction ΔEp from 60 mV at pH 0.8 up to 400 mV at pH 9, characteristic for a fast Nernstian electrode reaction and a slow electrode kinetic process, respectively.

A similar tendency is observed for the voltammetric behavior of hexacyanoferrate anion on the nonmodified mesoporous silica film electrode (Figure 3a, B). A decrease in the peak current of ca. 25% is observed in the whole range of pH, becoming more pronounced at pH above 6 because of the negative charging of the silica surface due to its deprotonation, in agreement with the pK_a of silica of 6.8.[36] The voltammetric response of the hexacanoferrate anion on the electrode coated with the nonmodified mesoporous silica film is characterized by much higher ΔEp values compared to those of the noncoated one, being 115 mV at pH 0.9 and gradually increasing up to 550 mV with increase in pH. This indicates that the nonmodified mesoporous silica film acts a partial barrier layer for the hexacyanoferrate anion. This is due to a decrease in the diffusion coefficient caused by the tortuosity of the diffusion pathway and to slowing down the electrode reaction kinetics. As will be shown later, this effect is, however, relatively small, and the nonfunctionalized silica films demonstrate good permeability for the hexacyanoferrate anions due to their well-developed and open porosity. The barrier effect of the nonmodified silica layer is only slightly dependent on pH.

Different pH-dependent electrode behavior is observed for the hexacyanoferrate anions on the electrode coated with an APTES-modified mesoporous silica film. According to the pH of the solution, amino groups are present either in the protonated form as $-NH_3^+$ or as neutral $-NH_2$, the pK_a of the NH_2/NH_3^+ pair equaling 5.7.[24] The degree of protonation of amino groups then substantially influences the permeation of hexacyanoferrate anions. Figure 3a, C, shows the marked effect of pH on the permeability of the aminofunctionalized mesoporous silica layer for hexacyanoferrate anions. At low pH values below pH 4, the response of the electrode coated with the amino functionalized silica layer exceeds that of the noncoated one. This points to the accumulation of anions within the positively charged layer due to the strong Coulomb interaction between the trivalent anions and the positively charged ammonium groups located within the pores so that the anion concentration in the silica layer exceeds that in the solution. Beyond pH of ca. 6 the permeability of the film for the anion drastically decreases, and at pH above 7 the surface of the electrode is practically closed for the anions in solution. This effect is stronger than expected from just the absence of electrostatic bonding and the decrease in the porosity, which was only 30% as determined from the equilibrium Kr adsorption data. This indicates that the kinetic processes are much more strongly affected by pore functionalization than the static ones such as the equilibrium Kr adsorption and points out that the anion diffusion to the electrode is hindered by the nonprotonated aminopropyl chains. A similar effect was observed by Soler-Illia et al. for the mesoporous titania layers modified with grafted organic groups.[37,38] They attributed the additional resistance

(34) Winkler, K. *J. Electroanal. Chem.* **1995**, *388*, 151.
(35) Huang, W. H.; McCreery, R. *J. Electroanal. Chem.* **1992**, *326*, 1.
(36) Iler, R. K. *The chemistry of silica*; J. Wiley & Sons: New York, 1978.
(37) Otal, E. H.; Angelome, P. C.; Bilmes, S. A.; Soler-Illia, G. *Adv. Mater.* **2006**, *18*, 934.

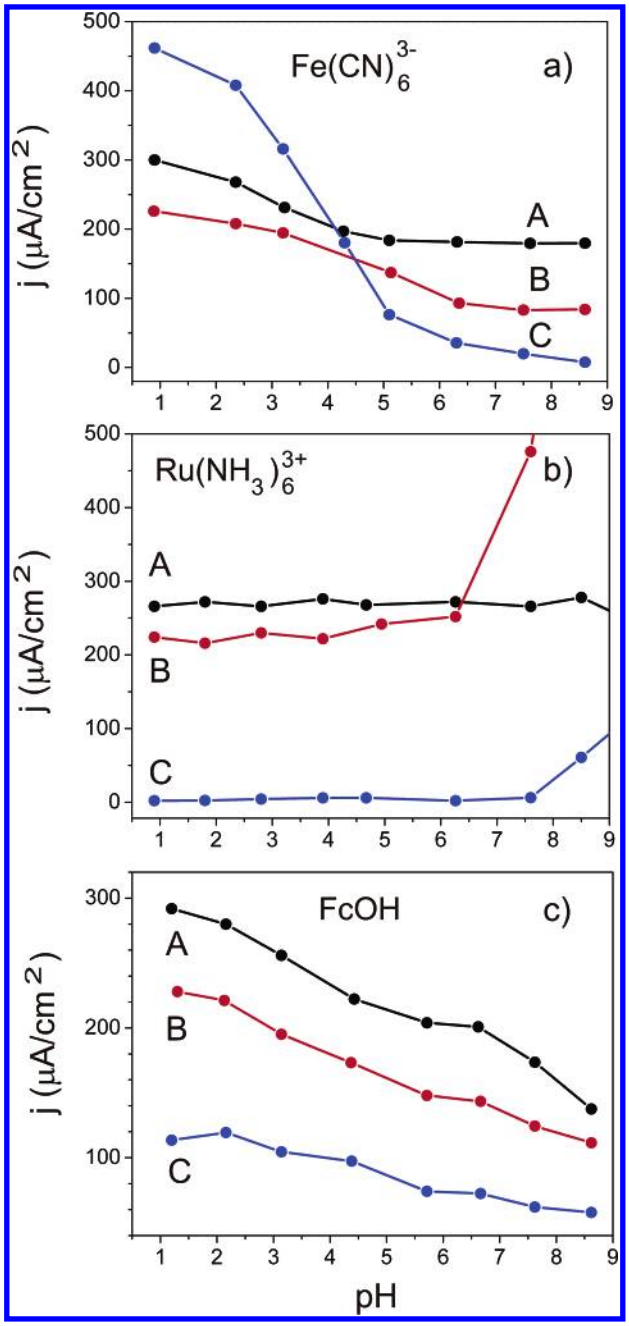

Figure 3. Voltammetric peak current at different pH in solutions of 1 mmol L^{-1} $Fe(CN)_6^{3-}$ (a), $Ru(NH_3)_6^{3+}$ (b), and ferrocenedimethanol (c) on the FTO electrodes: bare (A, black line); coated with nonfunctionalized (B, red line) and APTES-functionalized (C, blue line) mesoporous SiO_2 films.

of those groups to the diffusion of the charged species toward electrode to the pore wall−probe interactions influenced by polarity, hydrophilicity, and size of both pore modifiers and the permeate.

Hexaaminoruthenium Cations. In contrast to hexacyanoferrate anions, the electrode reaction of hexaaminoruthenium cations on bare FTO electrode is not influenced by pH; the peak current and potential peak difference of 60 mV remain constant in the whole tested pH range from 0.8 to 10.2 (Figure 3b, A). Coating of the electrode with the mesoporous silica film leads to a decrease in the peak current by less than 20% and some increase in the potential peak difference ΔEp to 75 ± 5 mV, the barrier effect being however smaller than for the hexacyanoferrate anions (Figure 3b, B). This is due to the residual negative charging of the silica surface, facilitating the permeation of the cationic species due to the electrostatic attractive interaction. At pH beyond 6.5, the negative excess charge of the silica surface leads to increased flux of $Ru(NH_3)_6^{3+}$ cations, and at pH above 8.5 the current exceeds by 3−6 times that on the noncoated electrode. However, at such high pH the substantially enhanced solubility of silica takes place, which leads to the irreversible damage of the silica layer. If pH of 8.5 is not exceeded, the mesoporous silica layer demonstrates the long-term stable membrane performance, as will be shown further.

The APTES-modified mesoporous silica layer operates for cations in the opposite way compared to the anions (Figure 3b, C). In the broad pH range of 0.8−7.5, such layer is closed for cations due to the repulsive electrostatic interactions of protonated amino groups and cationic hexaaminoruthenium species, the detected current being as low as only ca. 1% of that on the noncoated electrode. At pH above 7.5 the amino-modified silica layer becomes partially permeable for the cations; however, the observed current does not exceed 20% of that on the noncoated electrode in the working pH range below 8.5.

Ferrocenemethanol. Electrodes coated with mesoporous silica films demonstrate the same tendency in the voltammetric behavior observed for the ferrocenemethanol species on the bare FTO electrode, that is a gradual decrease in the peak current and increase in the peak potential difference with increase in pH (Figure 3c, A, B, C). The coating of the electrode surface with the mesoporous silica film leads to a decrease in the peak current by ca. 20% compared to the initial values in the whole pH range (Figure 3c, B). Aminofunctionalization of the silica film causes further decrease in the current values to 40% of that on the noncoated electrode, this value being independent of the pH (Figure 3c, C).

Comparison of the relative current change for all the tested redox probes on the amino functionalized mesoporous silica film electrode in the pH range of 0.8−10.5 is given in Figure 4. The membrane is closed for the cations at pH below 7.5 and remains permeable for the neutral ferrocenemethanol molecules in the whole range of pH. For hexacyanoferrate anions, the film is highly permeable at pH below 6 and is practically closed at higher pH. As the film permeability can be perfectly restored due to the subsequent decrease in pH, it operates as a switchable membrane layer, enabling one to control reversibly the anion flux by changing pH. It should be also stressed that the change in the current response is very fast, following the change in pH within some seconds, being much faster than the reported polymer layers, such as more than 10 min for the Ormosil membrane.[21,22] This is apparently due to the open porosity and low tortuosity of the mesoporous silica layers, which ensures the unhindered diffusion of the permeating species. The diffusion coefficients in the mesoporous silica films were calculated from the dependence of the peak current of the permeates on the applied scan rate according to $I_p = 2.69 \times 10^5 n^{3/2} A D^{1/2} C_O \upsilon^{1/2}$, where n is the number of transferred electrons (here 1), A is

(38) Angelome, P. C.; Soler-Illia, G. *J. Mater. Chem.* **2005**, *15*, 3903.

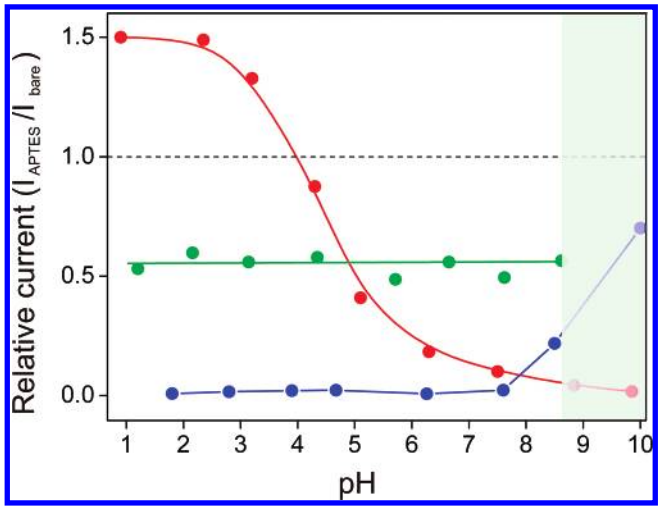

Figure 4. Relative change in peak current on the electrode coated with APTES-functionalized mesoporous SiO_2 layer in comparison to that on bare electrode (I_{APTES}/I_{bare}) at different solution pH for 1 mmol L^{-1} solutions of $Fe(CN)_6^{3-}$ (red line), $Ru(NH_3)_6^{3+}$ (blue line), and ferrocenedimethanol (green line). The gray zone marks the pH range where the irreversible electrode damage occurs due to the dissolution of the silica layer.

the electrode area, D is the diffusion coefficient, and C_O is the permeate concentration in the solution.[39] The diffusion coefficient D_p of ferrocenemethanol in the pores of the nonmodified and APTES-modified mesoporous silica film was found to be 1.8×10^{-6} cm^2 s^{-1} and 1.9×10^{-7} cm^2 s^{-1}, correspondingly, which is only 1.85 and 17 times smaller than the diffusion coefficient in the bulk-phase D_v of 3.3×10^{-6} cm^2 s^{-1}. The tortuosity factors τ can be then estimated as $\tau = \epsilon D_v/D_p$, where ϵ is the film porosity.[40] This gives the tortuosity factors of 1.1 and 6.8 for the nonmodified for the APTES-modified mesoporous silica films, correspondingly.

The very low tortuosity of the pristine mesoporous film indicates that the pore direction is not random (otherwise the tortuosity factor should be about 3), and the pore architecture has some degree of ordering.[41] This conclusion is in agreement with the electron microscopy and low-angle X-ray diffraction observations. The functionalization of the film surface has led to some increase in the tortuosity, however the pore system remains accessible and permeable for the ferrocenemethanol molecules.

The permselective membrane properties of the amino functionalized mesoporous silica films were tested for their use in the separation analysis. As can be seen from the Figure 5, the mixtures of differently charged analytes can be perfectly separated at low pH, at which the difference in the analyte permeation properties is most pronounced. It should be stressed that in spite of its open porosity and relatively large pores, such a membrane completely suppresses the flux of the cationic species to the substrate, at the same time enabling the permeation of the anionic or neutral species. This unique property, which is hardly realized for the dense membrane layers, can be especially advantageous for selective analysis of complex mixtures of both differently charged

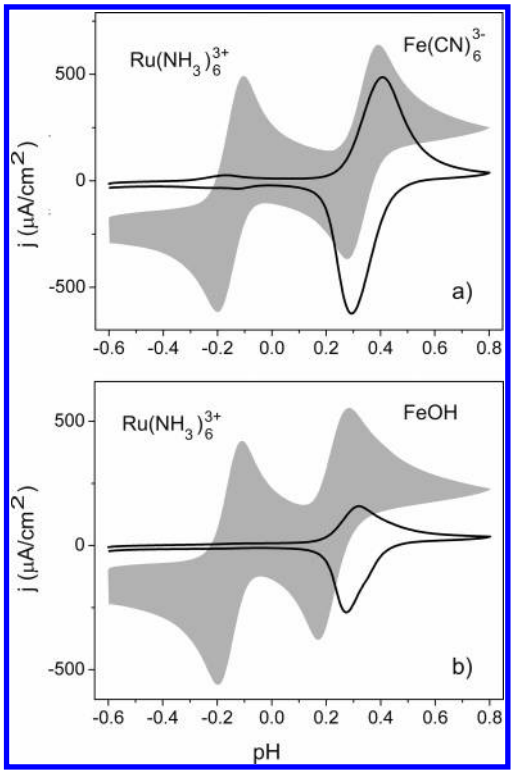

Figure 5. Cyclic voltammograms of equimolar mixture of $Ru(NH_3)_6^{3+}$ with $Fe(CN)_6^{3-}$ (a) and ferrocenedimethanol (b) on bare FTO electrode (gray area) and that coated with APTES-functionalized mesoporous SiO_2 film (black line). Analyte concentration, 1 mmol L^{-1}; pH of solution, 2.

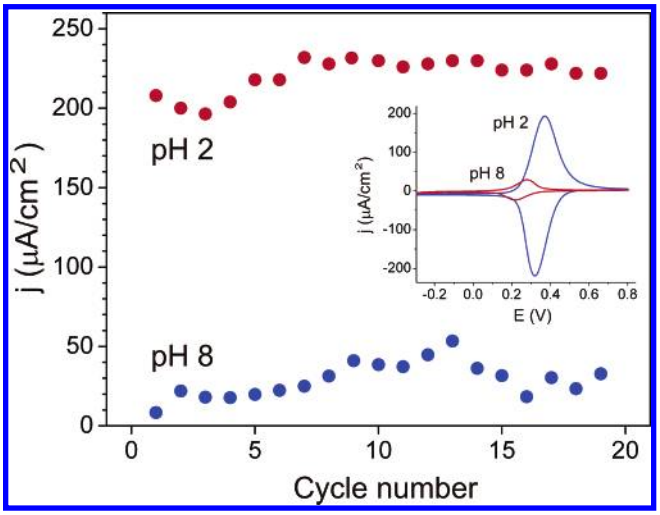

Figure 6. Reduction of the peak current of the electrode coated with an APTES-functionalized mesoporous SiO_2 layer in 1 mmol L^{-1} solution of $Fe(CN)_6^{3-}$ recorded at pH switched between 2 (red dots) and 8 (blue dots). The inset shows the corresponding cyclic voltammograms. The points corresponding to the 14−20th cycles were obtained after washing the electrode in a pure buffer solution (pH 8) without the redox probe.

and uncharged bulky analytes, where, e.g., only the neutral components should be detected. Mixtures of this kind are often encountered in biology and medicine, such as blood, urine, sera, etc. Switchable membranes could substantially enhance the performance of miniaturized biosensors with multiple function, which are highly promising devices with important application potential.

The long-term switching stability of such APTES-functionalized membranes was tested by the registration of the voltammetric response of 1 mmol L^{-1} $K_3Fe(CN)_6$ on a

(39) Bard, A. J.; Faulkner, L. R. *Electrochemical methods: fundamentals and applications*, 2nd ed.; J. Wiley & Sons: New York, 2001.
(40) Newton, M. R.; Morey, K. A.; Zhang, Y. H.; Snow, R. J.; Diwekar, M.; Shi, J.; White, H. S. *Nano Lett.* **2004**, *4*, 875.
(41) Suzuki, M. *Adsorption engineering*; Elsevier: Amsterdam, 1990.

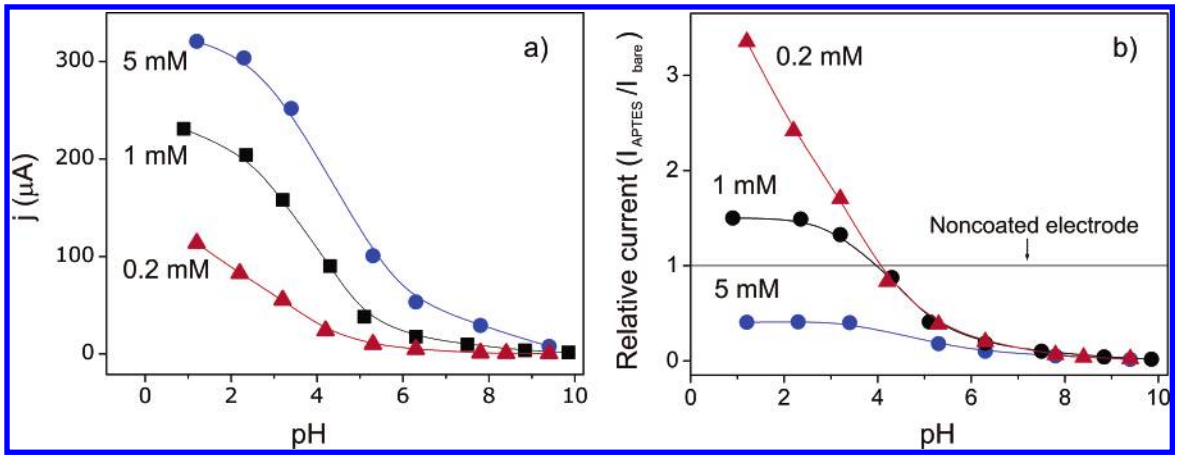

Figure 7. (a) Reduction in the peak current at different pH for 0.2, 1, and 5 mmol L^{-1} solutions of $Fe(CN)_6^{3-}$ on a FTO electrode coated with an APTES-functionalized mesoporous SiO_2 layer. (b) The same dependence represented as the relative change in current I_{APTES}/I_{bare} in comparison to that on a noncoated electrode.

membrane coated electrode at solution pH switched successively between pH 2 and pH 8 (Figure 6). At pH 2, the peak current of ca. 200 μA cm^{-2} was detected. It dropped to ca. 20 μA cm^{-2}, i.e., to 10% of the original value due to changing the solution pH to 8. Adjusting pH to 2 restored the current again to its initial value. The peak currents corresponding to two different pH values remained practically the same during at least 20 switching cycles (Figure 6). Some accumulation of the hexacyanoferrate anions in the membrane layer occurred after prolong switching (the point corresponding to the 13th cycle in the Figure 6); however, the permeation performance of the membrane is restored after washing in the pure buffer solution (pH 8) without the redox probe.

3.3. Permeation Mechanism of Amino-Functionalized Mesoporous Silica Films. The pH-controlled permeation properties of the APTES-functionalized mesoporous silica films (further "membrane") for the hexacyanoferrate anion were studied in a broad range of its concentration. For the $Fe(CN)_6^{3-}$ concentration ranging from 0.2 to 5 mM, the functionalized membrane is closed at high pH, while at low pH it is open and amplifies the flux of the anion, being practically a linear function of pH (Figure 7a). However, the amplifying effect of the membrane depends significantly on the anion concentration in the solution. While for the lowest concentration of 0.2 mmol L^{-1} the response of the membrane-coated electrode exceeds ca. 3.4 times that of the bare one, that is, the amplifying effect reaches 3.4; for anion concentration of 1 mmol L^{-1} the amplifying effect is subdued and achieves only about 1.5. For the highest anion concentration of 5 mmol L^{-1}, the current on the membrane-coated electrode is smaller than that on the bare one, and the membrane operates just as an anion flux regulator (Figure 7b).

The analysis of the voltammetric response of the membrane-coated electrode in differently concentrated $Fe(CN)_6^{3-}$ solutions is presented in Figure 8. For concentrations of 1 and 5 mmol L^{-1} at pH below ca. 2, the anion concentration at the electrode surface approaches some limiting value, which was estimated by multiplying the solution concentration by the membrane amplifying factor. As shown in the upper row of Figure 8, this "relative concentration" attains about 1.5−2 mmol L^{-1}, which can be considered as the maximum accumulation capacity of the membrane. For the lower concentration of 0.2 mmol L^{-1}, such saturation cannot be reached due to the insufficient amount of the solute. When this capacity exceeds the anion concentration in the solution, as is the case for 0.2 and 1 mmol L^{-1}, the amplifying effect of the membrane is observed due to the accumulation of the excess anions in the membrane and increase of the concentration gradient at the electrode surface. On the other hand, the membrane restricts the flux of the anions to the electrode surface if the concentration of the anions, which can be accumulated in the membrane, is lower than their concentration in the solution.

The kinetic regime of the electrode reaction at different pH of solution was determined by the analysis of dependence of peak current on the potential scan rate generally described as $I_p = f(v^n)$, providing the kinetic parameter $n = \partial \ln I_p/\partial \ln v$ (Figure 8, lower row). At low pH of solution, where the membrane accumulation capacity reaches its maximum, the kinetic parameter approaches 1, that is, current is linearly proportional to the scan rate. The voltammetric peaks have a symmetric nearly Gaussian shape, and the observed potential peak separation ΔEp values are much lower than 58 mV typical for the diffusion-controlled reversible electrode reaction, as low as 10 mV for the lower anion concentrations. Such current proportionality and peak characteristics are typical either for a reversible process controlled by the diffusion in a thin layer or for redox species immobilized on the electrode surface. For both mechanisms current $I_p = 9.39 \times 10^5 n^2 A \Gamma_O v$, where n is the number of electrons, A is the electrode area, D is the diffusion coefficient and Γ_O is surface coverage.[39] This kinetic mode is noted as *m1* in Figure 8. Although it is rather difficult to discriminate between two possible mechanisms, the observations of Soler-Illia at al[37] and our own study of electrochemical activity of modified mesoporous silica layers[31] point to the immobilized electrode-like behavior at low pH, enabling the hopping like electron transport between the $Fe(CN)_6^{3-}$ anions immobilized in the mesoporous layer at its maximum accumulation capacity.

At high pH the accumulation membrane properties are not observed any more, the proportionality factor n approaching

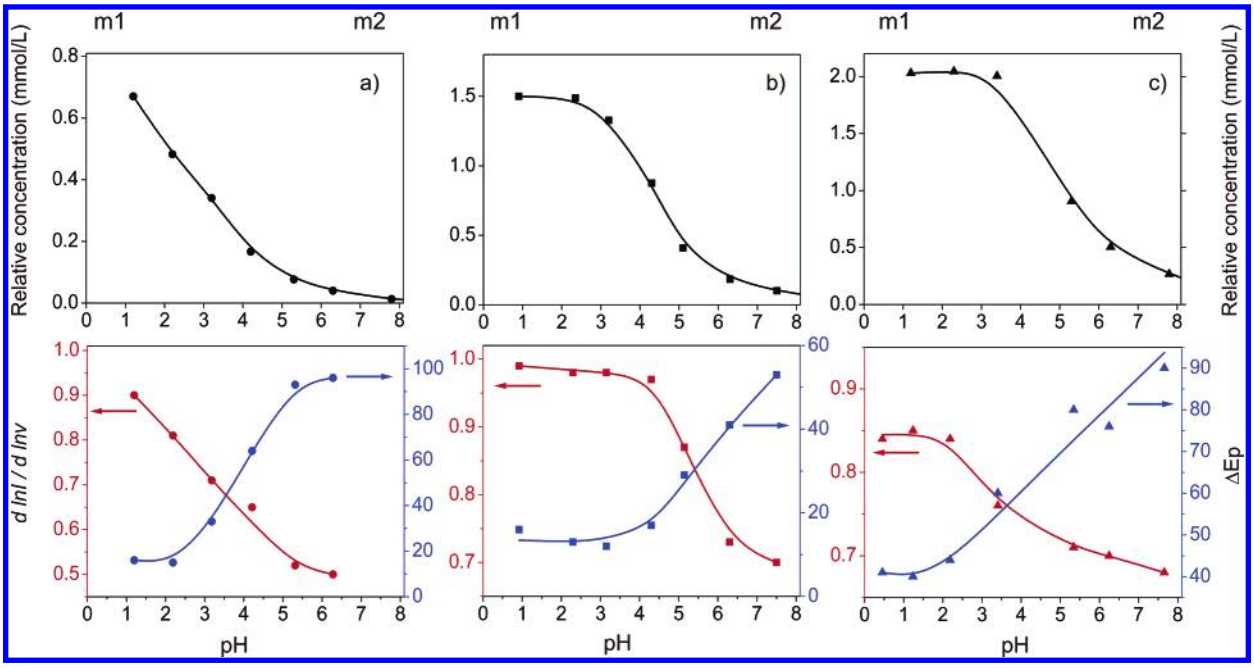

Figure 8. Analysis of voltammetric response at different solution pH of an electrode coated with an APTES-functionalized mesoporous SiO_2 layer in $Fe(CN)_6^{3-}$ solutions 0.2 mmol L^{-1} (a), 1 mmol L^{-1} (b), and 5 mmol L^{-1} (c) in concentration. Upper row: the relative concentration of $Fe(CN)_6^{3-}$ on the electrode surface estimated by the multiplication of the relative current I_{APTES}/I_{bare} and the solution concentration. Lower row: the current proportionality factor $\partial \ln I_p/\partial \ln \upsilon$ (red line, left axis) and the separation of the peak potential ΔEp for cathodic and anodic peaks (blue line, right axis).

0.5, i.e., the limiting current is proportional to the square root of the scan rate. The electrode reaction is thus controlled by the diffusion of the redox species toward the electrode described as $I_p = 2.69 \times 10^5 n^{3/2} A D^{1/2} C_O \upsilon^{1/2}$, and the potential peak separation ΔEp is equal or higher than 58 mV, typical for the diffusion-controlled reversible or quasireversible electrode process. This kinetic mode is noted as *m2* in the Figure 8.

Conclusions

In conclusion, the mesoporous SiO_2 layers functionalized with amino groups exhibit excellent permselective membrane properties, which allows one to control selectively the flux of the ions through the layers by changing pH. In spite of their open porous structure, such layers can completely block or enhance the flux of ions, depending on whether they are anions or cations, remaining at the same time semipermeable for the noncharged species.

In this article, only one type of the mesoporous silica films with a three-dimensional wormhole-like mesostructure and pore diameter of ca. 7 nm was used as a permselective membrane. However, the variety of such membranes can be significantly extended, and their performance toward desired ions can be easily optimized owing to the flexibility of the preparation procedure, as the used template-assisted sol−gel technique combined with postsynthetic modification enables one to obtain membranes with tailored porosity, pore size, and functionality. The developed preparation procedure is suitable for scaling up and applicable for a broad variety of supports. Moreover, the developed membranes exhibit very good mechanical and optical properties, which is often the Achilles' heel of materials for separation.

Acknowledgment. The work was supported by the Deutsche Forschungsgemeinschaft (projects WA 1116/10 and 436 TSE/113/46). We are grateful to Mrs. Kerstin Janze and Dr. Armin Feldhoff from the Institute of Physical Chemistry and Electrochemistry, Gottfried Wilhelm Leibniz Universität Hannover, for the SEM and TEM measurements.

Supporting Information Available: XRD pattern of mesoporous SiO_2. This material is available free of charge via the Internet at http://pubs.acs.org.

CM062389G